



Spring Succession and Vertical Export of Diatoms and IP₂₅ in a Seasonally Ice-Covered High Arctic Fjord

Audrey Limoges^{1,2*}, Guillaume Massé³, Kaarina Weckström^{1,4}, Michel Poulin⁵, Marianne Ellegaard⁶, Maija Heikkilä⁴, Nicolas-Xavier Geiffus⁷, Mikael K. Sejrrø⁸, Søren Rysgaard^{7,8} and Sofia Ribeiro¹

¹ Department of Glaciology and Climate, Geological Survey of Denmark and Greenland, Copenhagen, Denmark,

² Department of Earth Sciences, University of New Brunswick, Fredericton, NB, Canada, ³ Department of Biology, TAKUVIK, CNRS and Université Laval, Quebec, QC, Canada, ⁴ Ecosystems and Environment Research Programme, Environmental Change Research Unit, University of Helsinki, Helsinki, Finland, ⁵ Research and Collections, Canadian Museum of Nature, Ottawa, ON, Canada, ⁶ Department of Plant and Environmental Sciences, University of Copenhagen, Copenhagen, Denmark, ⁷ Centre for Earth Observation Science, Department of Environment and Geography, University of Manitoba, Winnipeg, MB, Canada, ⁸ Arctic Research Centre, Aarhus University, Aarhus, Denmark

OPEN ACCESS

Edited by:

Hauke Flores,
Helmholtz-Gemeinschaft Deutscher
Forschungszentren (HZ), Germany

Reviewed by:

Katrin Schmidt,
Plymouth University, United Kingdom
Gesine Mollenhauer,
Alfred Wegener Institute, Germany

*Correspondence:

Audrey Limoges
audrey.limoges@unb.ca

Specialty section:

This article was submitted to
Cryospheric Sciences,
a section of the journal
Frontiers in Earth Science

Received: 29 June 2018

Accepted: 26 November 2018

Published: 13 December 2018

Citation:

Limoges A, Massé G, Weckström K, Poulin M, Ellegaard M, Heikkilä M, Geiffus N-X, Sejrrø MK, Rysgaard S and Ribeiro S (2018) Spring Succession and Vertical Export of Diatoms and IP₂₅ in a Seasonally Ice-Covered High Arctic Fjord. *Front. Earth Sci.* 6:226. doi: 10.3389/feart.2018.00226

The biomarker IP₂₅ and fossil diatom assemblages preserved in seafloor sediments are commonly used as proxies for paleo Arctic sea-ice reconstructions, but how their production varies over the seasons and is exported to the sediment remains unclear. We analyzed IP₂₅ concentrations and diatom assemblages from a 5-week consecutive series of sea-ice cores and compared the results with sediment trap and surface sediment samples collected at the same site in the Young Sound fjord, Northeast Greenland. Our aim was to investigate the dynamics of diatom colonization of the spring sea ice and the *in situ* production of IP₂₅. Additionally, selected diatom taxa observed in the sea-ice samples were isolated from in-ice assemblages and their lipid composition was analyzed via gas chromatography-mass spectrometry. We confirm that *Haslea spicula* (and not the closely related species *H. crucigeroides*) is an IP₂₅-producer. All three known IP₂₅-producing taxa (*Haslea spicula*, *H. kjellmanii*, and *Pleurosigma stuxbergii* var. *rhomboides*) were present in Young Sound sea-ice and the low IP₂₅ concentrations measured in the sea-ice (0.44–0.72 pg mL⁻¹) were consistent with the low abundance of these source species (0.21–9.66 valves mL⁻¹). Total sympagic diatom production also remained very low (21–985 valves mL⁻¹), suggesting that the fjord's sea ice did not provide an optimal physical-chemical environment for diatoms to thrive. Temporal changes in the sympagic diatom community were also observed, with an early presence of the pelagic *Thalassiosira hyperborea* and subsequent dominance of pennate taxa, including *Nitzschia* and *Navicula* species, *Fossula arctica* and *Stauronella arctica*. The assemblages observed during and after the seasonal ice melt consisted primarily of *Fossula arctica*, *Fragilariopsis oceanica*, *Thalassiosira antarctica* var. *borealis* (resting spores), and *Chaetoceros* spp. (vegetative cells and resting spores). The seafloor sediment assemblages largely reflected the melt and post-melt planktic production and were dominated by the resting spores of the centric *Chaetoceros* spp. and *Thalassiosira*

antarctica var. *borealis*, and the pennate *Fragilariopsis oceanica*, *Fossula arctica*, and *Fragilariopsis reginae-jahniae*. This study documents that IP₂₅ is produced in Young Sound, and that the weak fingerprint of sea ice in the sediment appears to be primarily due to the limited sea-ice diatom biomass.

Keywords: climate change, Arctic sea-ice, HBIs, diatoms, paleoenvironmental reconstructions, climate proxy, Northeast Greenland

INTRODUCTION

The reliable reconstruction of past sea-ice variability in polar regions is a key prerequisite for climate model development. Due to its effects on the Earth's radiative properties (e.g., Curry et al., 1995), ocean heat transport (e.g., Jahn and Holland, 2013; Tomas et al., 2016), and the stability of tidewater outlet glaciers (e.g., Bendtsen et al., 2017), the rapid sea-ice decline associated with current climate warming can contribute to further changes in the climate system (e.g., Serreze and Barry, 2011). Our ability to fully evaluate and comprehend these impacts is however impaired by the scarcity and short time span of monitoring data. This paucity of long-term information about the interactions between climate and sea ice has motivated the development of methods that are based on the study of tracers preserved in seafloor sediments. Thorough reviews of sea-ice proxies, including their strengths, and shortcoming are presented in Polyak et al. (2010) and de Vernal et al. (2013). Proxy records enable us to extend sea-ice data several millennia back in time and make it possible to define environmental variability at a (multi-) decadal resolution.

The bottom horizon of sea-ice, in particular the 1–3 cm above the ice-water interface (Brown et al., 2011), forms the habitat of diatom species that produce a fossilizable molecular biomarker, IP₂₅ (Ice Proxy with 25 carbon atoms; Belt et al., 2007), and sedimentary IP₂₅ quantifications have become a widely-applied approach to reconstruct past seasonal sea-ice conditions in the Northern Hemisphere (e.g., Massé et al., 2008; Andrews et al., 2009; Vare et al., 2009; Belt et al., 2010; Müller et al., 2012; Cabedo-Sanz and Belt, 2016). This mono-unsaturated highly branched isoprenoid (HBI) alkene is biosynthesized in the sea-ice matrix by a restricted number of common pan-Arctic diatoms belonging to the *Haslea* and *Pleurosigma* genera (Brown et al., 2014) and is deposited in underlying sediments when the ice melts, in spring, or summer. The source-specific nature and high preservation potential (see however Rontani et al., 2018) of this organic molecular compound makes it a useful biomarker for the reconstruction of past sea-ice conditions. Additionally, since the frustules of sympagic diatoms are generally weakly silicified and do not preserve well in the sediment, IP₂₅ constitutes one of the rare direct lines of evidence for the past presence of annually formed sea ice. In fully marine settings, high levels of sedimentary IP₂₅ content are generally reported to reflect long-lasting seasonal sea-ice, polynya, or marginal ice zone conditions, whereas the absence of IP₂₅ can either indicate perennial sea-ice cover or open water (e.g., Belt and Müller, 2013). Downcore changes in the sedimentary IP₂₅ concentrations from a given location are therefore typically interpreted to reflect temporal fluctuations in the sea-ice conditions.

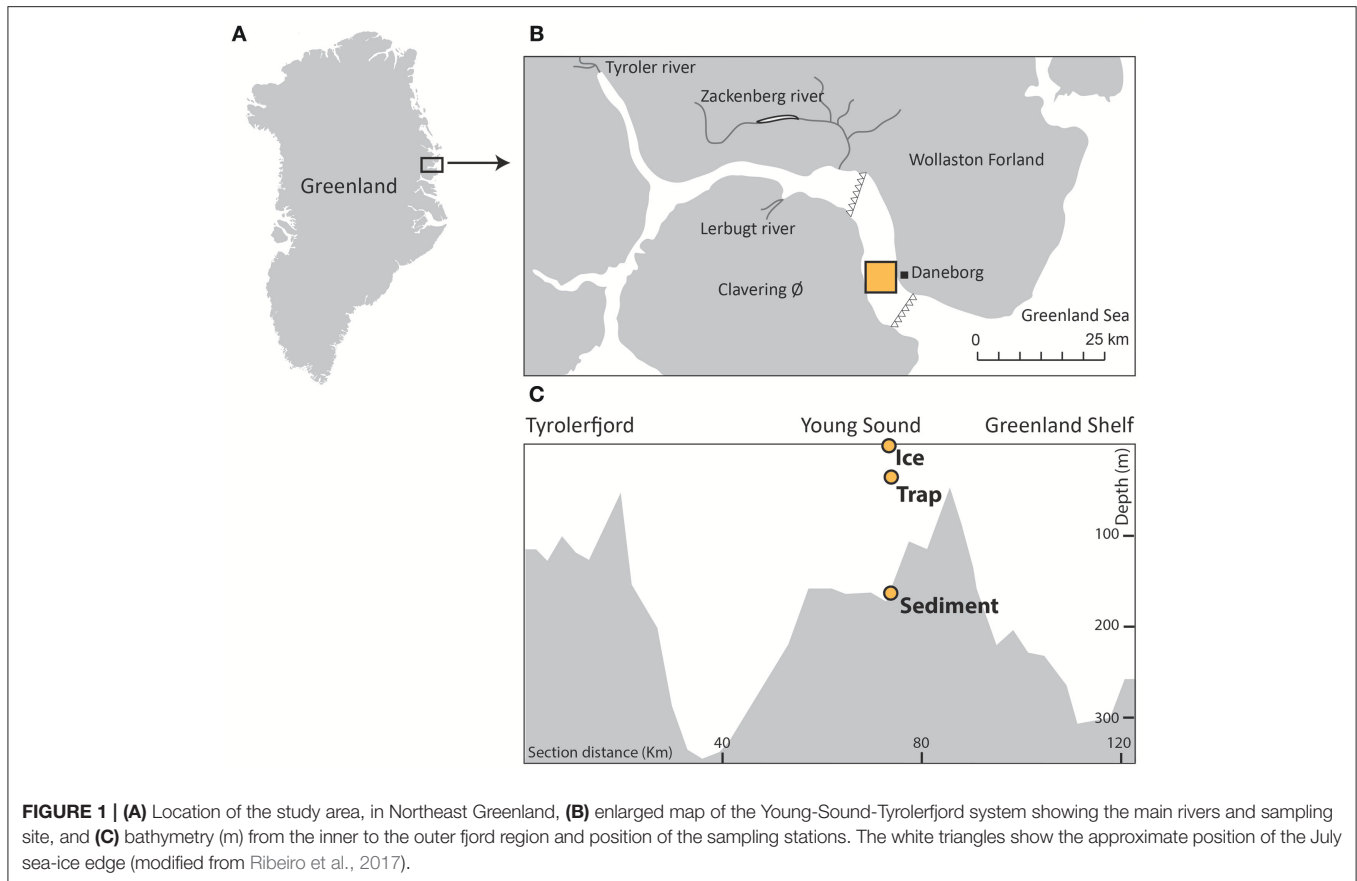
However, recent studies have shown that the sedimentary concentrations of IP₂₅ in coastal areas influenced by freshwater runoff are lower than expected, thus showing a mismatch with overlying sea-ice cover extent (Xiao et al., 2013; Hörner et al., 2016; Ribeiro et al., 2017; Limoges et al., 2018). Despite the growing number of IP₂₅-based sea-ice reconstructions, only a limited number of studies have, to date, investigated the ecophysiological and environmental parameters that determine IP₂₅ production (e.g., Brown et al., 2011, 2014), raising concerns about the interpretation of IP₂₅ as a quantitative indicator of sea-ice cover, and the possible limitations to its application in the Arctic (Belt and Müller, 2013).

Here, we present a two-step investigation based on (1) biomarker and diatom analyses of sea-ice cores, sediment trap, and seafloor sediment samples from the Young Sound, a high Arctic fjord located in northeastern Greenland, and (2) targeted diatom culture experiments. The Greenland Ecosystem Monitoring (GEM) programme has carried out systematic measurements in the Young Sound–Tyrolerfjord system since 2003 (Rysgaard and Glud, 2007), providing a robust record of the variability in environmental conditions (e.g., irradiance, salinity) which can be reproduced in the laboratory. This approach provides valuable insight into (i) the IP₂₅ production in spring sea-ice, (ii) temporal trends in spring diatom assemblage composition and abundance in the sea ice, (iii) vertical transfer of diatom valves and IP₂₅ from ice to sediments, and (iv) production of HBIs by a selection of sympagic diatom species. This study aims to improve paleoenvironmental interpretations for the Arctic region based on diatom-derived proxies.

ENVIRONMENTAL SETTING

The Young Sound is located in northeastern Greenland (74°N – 20°W) (Figure 1) and, together with the Tyrolerfjord, forms a ca. 90 km long, and 2–7 km wide fjord system connected to the Greenland Sea. Along the eastern shelf of Greenland, the coastal waters are influenced by the East Greenland Current, which consists of Polar Surface Waters of low temperature (< 0°C), and salinity (<34.4‰), overlying relatively warmer (0–2°C), saline (>34‰), Atlantic waters (>150 m depth) (Boone et al., 2018). In the fjord system, however, a shallow sill of ca. 45 m depth located at the entrance to the fjord forms a natural topographic barrier that prevents the entrainment of more saline Atlantic waters.

The transmittance of light into the surface-waters is attenuated by sea ice and the overlying snow from ca. late-October to mid-July (Figure 2). In late July, any remaining sea ice is typically flushed out of the fjord. The duration of the ensuing open-water season has increased since 2000 and currently lasts



~3 months, until late October or early November. A continuous time series of temperature and salinity in the vicinity of our study location is presented in Boone et al. (2018) and underlines a stepwise freshening of the fjord's subsurface and deep waters from 2003 to 2015 (see also Sejr et al., 2017). The fjord's hydrography also experiences important seasonal variation in salinity, with values ranging from 17 to 33.4‰, and 32.25 to 32.50‰, respectively, in the summer, and winter of 2013–2014 (Boone et al., 2018). Both the seasonal sea-ice melt and river runoff ($0.63\text{--}1.57\text{ km}^3\text{ yr}^{-1}$; Mernild et al., 2007) contribute to the formation of a shallow surface lens of fresher water (5–10 m; $S < 25\text{‰}$) from the end of June to July (Rysgaard et al., 1999; Sejr et al., 2017). In August, the sediment discharge associated with the Tyroler, Lerbugt, and Zackenberg rivers creates turbid plumes that cause poor light conditions, especially in the inner part of the fjord (Kroon et al., 2017; Ribeiro et al., 2017) (see **Figure 1**). The Zackenberg river alone can discharge sediment loads of the order of $16.1\text{--}130 \times 10^6\text{ kg yr}^{-1}$ (Jensen et al., 2014).

Sea-ice algal productivity is very low and only represents <1% of the total annual pelagic primary production in the fjord (Rysgaard et al., 2001). Monitoring of the summer planktic protist communities across the Young Sound–Tyrolerfjord system from 2009 to 2012 revealed clear spatial and temporal heterogeneities in the assemblages, largely associated with the strong gradients in surface temperature, and salinity within the system (Krawczyk et al., 2015). Diatoms were

generally the most important group within the assemblages and as such play a predominant role in the fjord's primary production.

MATERIALS AND METHODS

Sea-ice Core Samples

Multiple cores of landfast first-year ice were retrieved from the outer part of the Young Sound, near the Daneborg research station ($74^\circ 18.979'N, 20^\circ 17.623'W$) (**Figure 1**) over five consecutive weeks during Spring 2014, using a SIPRE corer of 7.6 cm diameter. Sea ice temperature was measured *in-situ*, immediately after extraction of the ice cores using a calibrated temperature probe (Testo 720, $\pm 0.1^\circ\text{C}$ precision) inserted into pre-drilled holes (2.5 cm intervals), perpendicular to core sides. Bulk sea-ice salinity was determined on melted sea-ice sections using a calibrated Thermo Scientific Orion portable salinometer WP-84TPS with a precision of ± 0.1 . Salinity is reported on the psu scale (practical salinity scale). *In-situ* temperature and salinity measurements for the bottom 10 cm of the ice cores are shown in **Figure 3**. In line with the progressive seasonal ice melt, core lengths decreased from 1.43 m in 26 May to 1.33 m in 23 June (**Table 1, Figure 3**). Concomitantly, snow cover thickness steadily declined from 61 to 14 cm over the same period (**Table 1, Figure 3**). The last core was collected ~1 month before the ice break-up. Ice

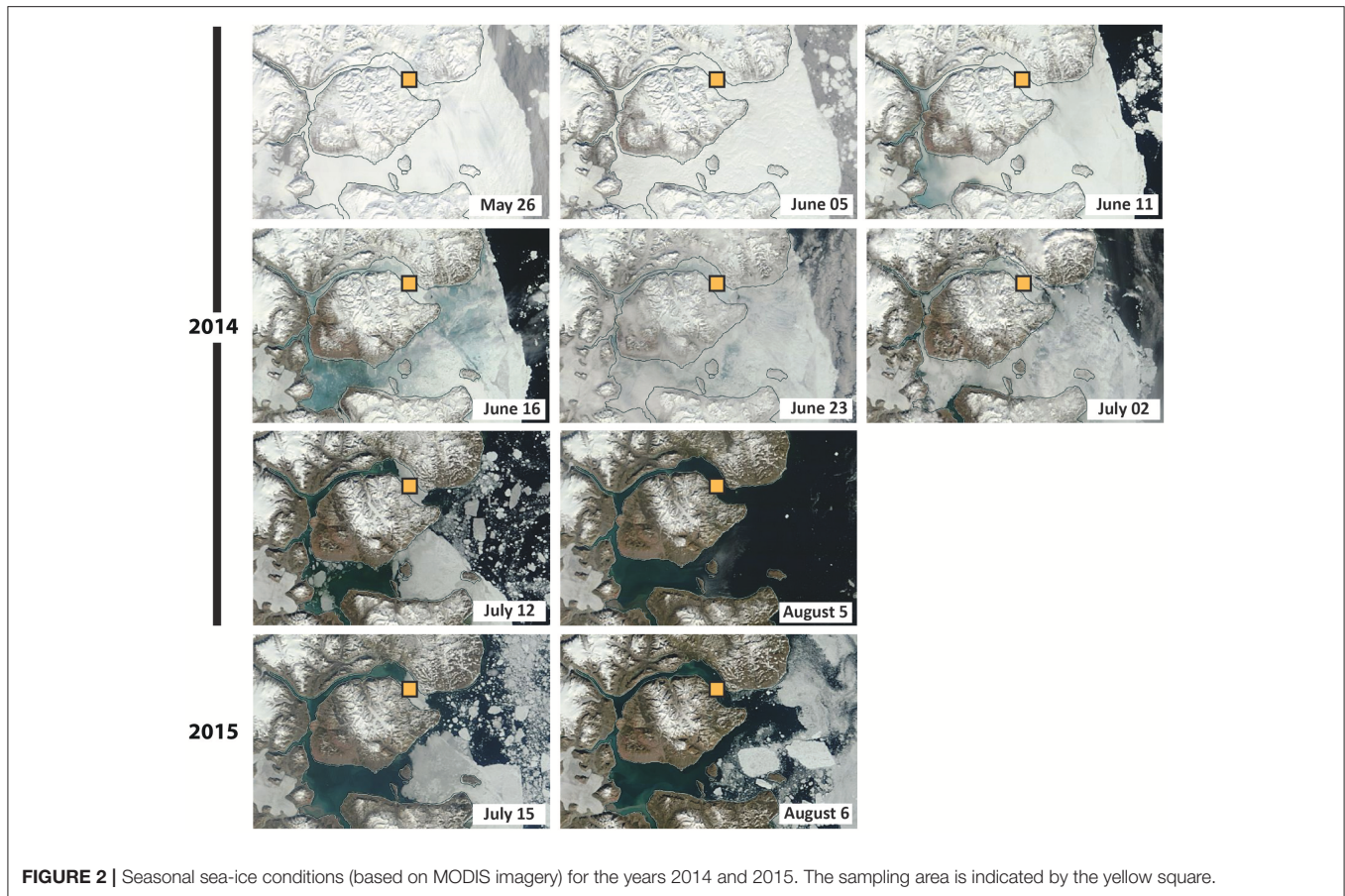


FIGURE 2 | Seasonal sea-ice conditions (based on MODIS imagery) for the years 2014 and 2015. The sampling area is indicated by the yellow square.

core samples were transported from Greenland and stored at -80°C , at the Arctic Research Center, in Aarhus University until processed.

The bottom 10 cm of the ice cores was melted in glass beakers and placed in a refrigerator at 4°C and in the dark for 24 h. When possible, replicates of the ice cores were pooled together (Table 1). In the samples reserved for taxonomic examinations, cells were allowed to settle onto the bottom of the beakers, and fixed with acidic Lugol's solution. For the IP₂₅ analyses, melted samples were filtered through a Whatman GF/F 47 filter, and the filters frozen at -80°C .

Trap and Seafloor Sediments

A PPS4/3 sediment trap with automated year-round sampling was deployed at 37 m (74.322°N 20.269°W) at the GEM Program (Figure 1C). Prior to launching, the collector cups were filled with Whatman GF/F filtered seawater, mercuric chloride (HgCl_2), and adjusted to a salinity of 40 ‰ using a solution of sodium chloride (NaCl). The mean current velocity at the trap location is lower than 2 cm s^{-1} (Rysgaard et al., 2003), therefore permitting an efficient trapping of sinking particles. For preservation purposes, HgCl_2 was also added after sample recovery (see sampling manual MarineBasis program; Rysgaard et al., 2009). Samples were stored in a cool room (4°C) until analysis.

The time intervals of interest for this study covered by the sediment trap samples are as follows: (1) 24 April to 3 June 2014; (2) 1 July to 4 August 2014, and (3) 15 July to 4 August 2015. As such, the first sediment trap collected sinking particles before the ice melt, and the two others provide a comparison of the particles that were trapped during, and after the ice melt of both 2014 and 2015.

For comparison, we used the topmost (0–1 cm) interval of a sediment core collected in 2014 from 163 m water depth (Rumohr lot core number YS163_R1, collected at 74.3097°N , 20.3°W) (Figure 1C). The sediment was freeze-dried and kept at -80°C until further processing. The IP₂₅ data from this site is given by Ribeiro et al. (2017, site YST2).

Culture Experiment

Individual diatoms were isolated from natural sea-ice samples (bottom 5 cm of sea-ice cores) collected from Churchill in Hudson Bay, Manitoba in 2005, and Allen Bay, near Resolute Bay, Nunavut in 2013. The sea-ice cores were drilled with a Kovacs Mark III corer of 9 cm diameter. The bottom 5 cm were sectioned using a stainless-steel surgical saw and placed in a cooler with $0.2\text{ }\mu\text{m}$ filtered seawater and stored in the dark below 4°C until the ice melted. Single cells were isolated under the microscope and placed in culture plates filled with Guillard F/2 enriched seawater. Plates were then stored in a cooled (0°C)

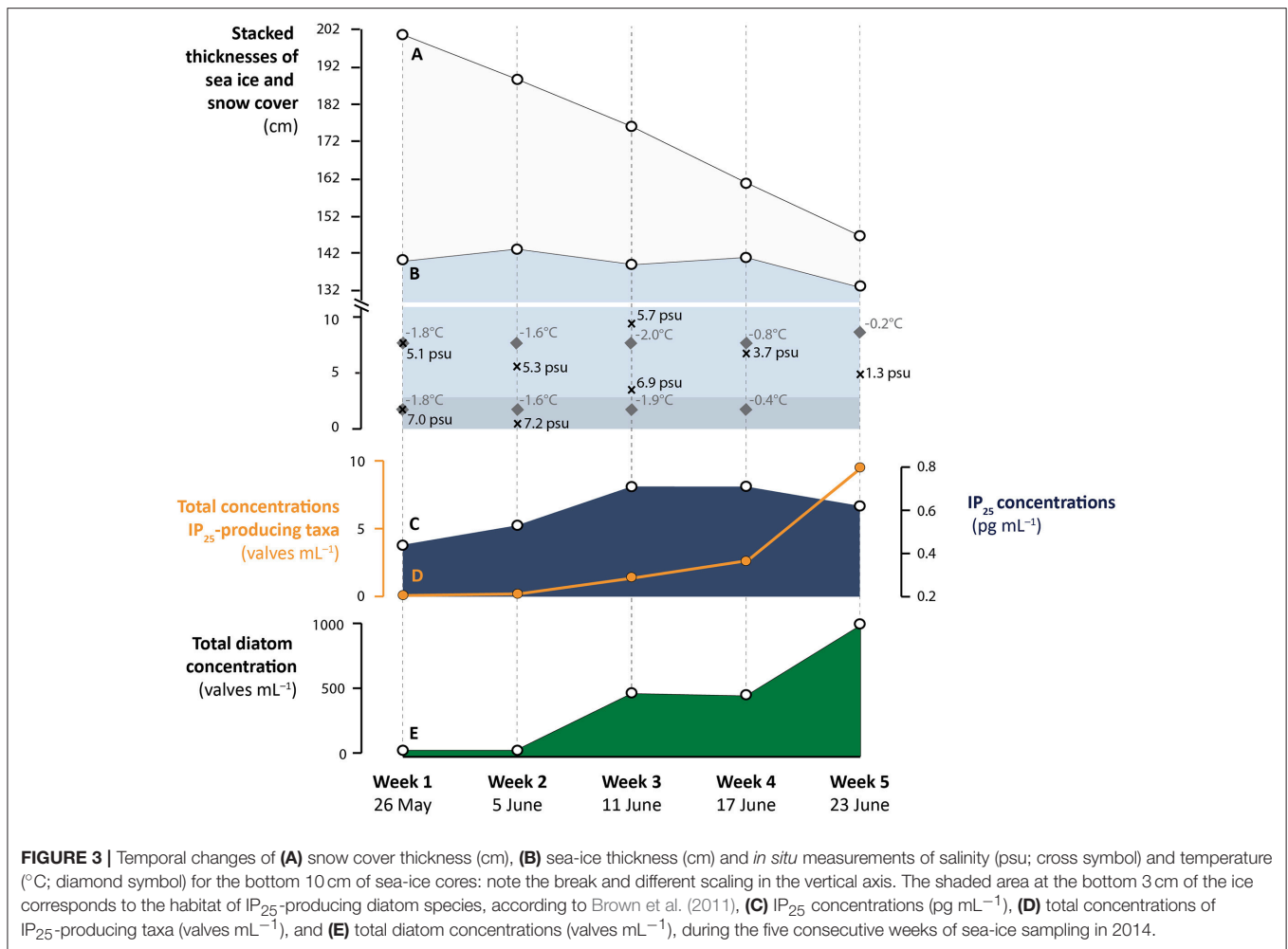


FIGURE 3 | Temporal changes of (A) snow cover thickness (cm), (B) sea-ice thickness (cm) and *in situ* measurements of salinity (psu; cross symbol) and temperature (°C; diamond symbol) for the bottom 10 cm of sea-ice cores: note the break and different scaling in the vertical axis. The shaded area at the bottom 3 cm of the ice corresponds to the habitat of IP₂₅-producing diatom species, according to Brown et al. (2011), (C) IP₂₅ concentrations (pg mL⁻¹), (D) total concentrations of IP₂₅-producing taxa (valves mL⁻¹), and (E) total diatom concentrations (valves mL⁻¹), during the five consecutive weeks of sea-ice sampling in 2014.

plant culture chamber during several weeks until sufficient cells were obtained to transfer the culture into a 250 mL Erlenmeyer flask containing 125 mL of F/2 enriched seawater (salinity of 30‰). After some weeks, sufficient biomass was obtained to carry out both taxonomic identification and hydrocarbon analysis. Cells from each flask were then re-suspended using magnetic stirrers and a 50 mL aliquot filtered using GF/F filters. Filters were then inserted in an 8 mL glass vial and stored at -20°C until analysis. The lipid composition of the different species was determined following the method described in section Biomarker analysis. Results presented here refer specifically to the diatom taxa that were identified in the sea-ice samples from both Canada (Manitoba, Nunavut) and Greenland (Young Sound).

Diatom Identification and Quantification

Three endemic diatom species/species complexes responsible for the production of the lipid IP₂₅ were identified by Brown et al. (2014): *Pleurosigma stuxbergii* var. *rhomboides*, *Haslea kjellmanii*, and *Haslea crucigeroides*, and/or *H. spicula*. Due to their morphological similarity, it was not possible during the experiment undertaken by Brown et al. (2014) to determine whether both *H. crucigeroides* and *H. spicula* produce IP₂₅.

These two pennate diatoms both have lanceolate valves. The variation in valve width between *H. crucigeroides* and *H. spicula* is 13–17 μm and 7–10 μm, respectively. The shape of the distal parts of their valves is also different: *H. crucigeroides* has sub-rostrate beak-like ends, while *H. spicula* has acutely rounded or pointed ends. Furthermore, the number of transapical striae in 10 μm differs between the two species: *H. spicula* has 25–30 striae in 10 μm, while *H. crucigeroides* has ca. 20–24 striae in 10 μm (Hustedt, 1961; Snoeijs, 1993; Snoeijs and Vilbaste, 1994; Snoeijs and Potapova, 1995; Snoeijs and Kasperoviciene, 1996; Snoeijs and Balashova, 1998; Witkowski et al., 2000). The striation in *Haslea* is characterized by a transapical pattern crossed at right angle by a longitudinal pattern. Therefore, there are 18–22 transapical and 21–28 longitudinal striae in *H. crucigeroides*, and 25–30 transapical and >40 longitudinal striae in *H. spicula*. The literature reported only refers to light microscope observations; the range of striae above are from SEM examination of Arctic sea-ice samples (M. Poulin, personal observation). To resolve the morphological differences between *H. crucigeroides* and *H. spicula*, droplets of sea-ice samples were examined using a scanning electron microscope (SEM; Environmental SEM Quanta 200, FEI). Aliquots of the original

TABLE 1 | Sampling date, ice and snow thicknesses (cm), number of sea-ice core replicates and corresponding total volume filtered for IP₂₅ measurements, number of sea-ice core replicates and corresponding initial volume used for diatom counts, and total concentrations of diatoms, IP₂₅-producing diatom taxa, *Haslea spicula*, *H. kjellmanii* and *Pleurosigma stuxbergii* var. *rhomboides* (valves mL⁻¹ or valves g⁻¹) and IP₂₅ concentration (pg mL⁻¹ or ng g⁻¹) corresponding to the sea-ice, sediment trap and surface sediment samples.

Sampling date	Ice thickness (cm)	Snow thickness (cm)	Number sea-ice replicates IP ₂₅	Volume filtered for IP ₂₅ measurements (mL)	Number sea-ice replicates diatom counts	Initial volume samples for diatom counts (mL)	Total diatom concentration (valve mL ⁻¹)	Total IP ₂₅ -producing taxa concentration (valve mL ⁻¹)	Concentration <i>H. spicula</i> (valve mL ⁻¹)	Concentration <i>H. kjellmanii</i> (valve mL ⁻¹)	Concentration <i>P. stuxbergii</i> var. <i>rhomboides</i> (valve mL ⁻¹)	IP ₂₅ concentrations (pg mL ⁻¹)
SI-W1 26 May 2014	140	61	2	1080	1	575	21	0.21	0.10	0.00	0.10	0.4 ± 0.2
SI-W2 5 June 2014	143	46	4	2375	2	500	26	0.33	0.33	0.00	0.00	0.5 ± 0.05
SI-W3 11 June 2014	139	37.5	4	2475	2	600	459	1.49	0.00	1.49	0.00	0.7 ± 0.03
SI-W4 17 June 2014	141	20	4	1615	2	550	441	2.78	2.78	0.00	0.00	0.7 ± 0.1
SI-W5 23 June 2014	133	14	4	2430	2	630	985	9.66	9.66	0.00	0.00	0.6 ± 0.05

Sampling interval		Total concentration IP ₂₅ -producing taxa (valve g ⁻¹)	Concentration <i>H. spicula</i> (valve g ⁻¹)	Concentration <i>H. kjellmanii</i> (valve g ⁻¹)	Concentration <i>P. stuxbergii</i> var. <i>rhomboides</i> (valve g ⁻¹)	IP ₂₅ concentrations (ng g ⁻¹)
TS1	24 April–3 June 2014	0	0	0	0	Not analyzed
TS2	1 July–4 August 2014	0	0	0	0	Not analyzed
TS3	15 July–4 August 2015	0	0	0	0	Not analyzed

Site		Total concentration IP ₂₅ -producing taxa (valve g ⁻¹)	Concentration <i>H. spicula</i> (valve g ⁻¹)	Concentration <i>H. kjellmanii</i> (valve g ⁻¹)	Concentration <i>P. stuxbergii</i> var. <i>rhomboides</i> (valve g ⁻¹)	IP ₂₅ concentrations (ng g ⁻¹)
YST2		0	0	0	0	20.69

sea-ice samples were dehydrated through a graded series of ethanol and critical point dried. The samples were then mounted on aluminum stubs and coated with a gold/palladium mixture (instrument: FISONs, Polaron SC7640).

Species identification and cell counts were also carried out in light microscopy (Leica DMLB) at 1000× magnification. Sea-ice samples were prepared following the procedure described in Lundholm et al. (2002). Samples were oxidized using hydrogen peroxide (H₂O₂ 30%) and a saturated aqueous solution of potassium permanganate (KMnO₄) in order to remove organic material. After 24 h, samples were cleared by addition of a saturated aqueous solution of oxalic acid (COOH₂) and then washed several times with distilled water. Total sea-ice diatom concentrations were determined by addition of sample aliquots to a Sedgewick-Rafter counting chamber.

Permanent diatom microscope slides were prepared from the trap and surface sediment samples, following standard methodologies (Battarbee et al., 2001). These are stored at the Geological Survey of Denmark and Greenland and available upon request. In brief, the sediment was treated with hydrogen peroxide (H₂O₂, 30%) and hydrochloric acid (HCl, 25%) in order to remove the organic material and carbonates, respectively. The test tubes in which samples were treated were subsequently filled with distilled water and left to settle for 12 h. Residues were then washed (and left to settle) several times using demineralized water. A few drops of the final suspension were allowed to dry on a cover slip and subsequently mounted in Naphrax™ for observation. Identification and quantification of diatom valves were performed in light microscopy (Leica DMLB) using phase contrast optics, at a 1000x magnification.

In order to assess the degree of similarity between the diatom assemblages from the sea-ice, sediment traps, and surface sediment samples, classical cluster analysis using an unweighted pair-group average (UPGMA) clustering algorithm and a Euclidean similarity index was carried out using the software PAST3.12 (Hammer et al., 2001).

Biomarker Analysis

Samples for IP₂₅ analysis were processed following the protocol described by Belt et al. (2007). An internal standard (7-hexylnonadecane) was added to the melted ice sample and to ~0.5 g of the freeze-dried and homogenized sediment samples before analytical treatment. For both sample types, total lipids were ultrasonically extracted (3 times) using a mixture of dichloromethane (DCM: CH₂Cl₂) and methanol (MeOH) (2:1, v/v). Extracts were pooled together, and the solvent was removed by evaporation under a slow stream of nitrogen. The total extract was subsequently suspended in hexane and purified through open column chromatography (SiO₂). HBI isomers were eluted using hexane (8 mL). Procedural blanks and standard sediments were analyzed every 15 samples.

Hydrocarbon fractions were analyzed using an Agilent 7890 gas chromatograph (GC) fitted with 30 m fused silica Agilent J&C GC columns (0.25 mm internal diameter and 0.25 μm phase thickness) and coupled to an Agilent 5975C Series mass selective detector. Oven temperatures were programmed as follows: 40–300°C at 10°C min⁻¹, followed by an isothermal interval at

300°C for 10 min. The data were collected using ChemStation and analyzed using MassHunter quantification software. IP₂₅ was identified on the basis of retention time and comparison of mass spectra with authenticated standards. Abundances were obtained by comparison of individual GC-mass spectrometry responses against those of the internal standard and concentrations are reported in pg mL⁻¹ and ng g⁻¹ for the ice and sediment samples, respectively. Response factors of the internal standard vs. IP₂₅ were determined prior and after each analytical sequence (every 15 samples). The extraction and analytical error on the measurements, determined from measurements of standard sediments is of ± 8%.

RESULTS

Culture Experiments

Thirteen of the diatom taxa observed in the sympagic assemblages from Young Sound were isolated from natural sea-ice samples. These included some of the taxa that typically dominate Arctic sea-ice assemblages (e.g., *Nitzschia frigida*; Poulin et al., 2011). The hydrocarbon composition of all 13 taxa was analyzed (Table 2). The IP₂₅ compound was only identified in cultures of the diatom *H. spicula*. Analysis of their hydrocarbon fractions indicates that *H. crucigeroides* and *H. vitrea* do not produce IP₂₅, but C₂₅ tri- and quadri-unsaturated HBI isomers (Figure 4). For all the other diatom taxa analyzed, neither IP₂₅, nor other HBI isomers were detected (Table 2).

Sea-ice Diatom Succession and IP₂₅ Production

In total, 55 diatom taxa belonging to 24 genera were identified in the ice samples (Supplementary Material). Total sea-ice diatom concentrations increased from ca. 21 valves mL⁻¹ on 26 May to 985 valves mL⁻¹ on 23 June (see Table 1, Figure 3). The rate of increase was not constant and appeared to be driven in part by changes in sea-ice thickness during the sampling period. The low diatom concentration suggests that the initial stages of sympagic productivity were captured by the first ice samples. The subsequent increase in diatom cells was accompanied by marked changes in the community composition (Figure 5). From 26 May to 5 June, the sea-ice assemblages were dominated by centric taxa, notably *Thalassiosira hyperborea* (50% of the assemblage). Dominant taxa also included *Navicula* (17%) and *Nitzschia* (10%) species (see Table 2 for complete species list). The relative contribution of the centric diatoms then decreased drastically from 11 June, when *Nitzschia frigida* reached a relative abundance of 76%. On 17 June, the assemblages were dominated by *Nitzschia frigida* (37%), *Navicula* spp. (32%), and *Fossula arctica* (10%). Finally, on 23 June, *Nitzschia* spp. was still abundant but the assemblages were largely dominated by *Stauronella arctica* (72%), which had only contributed to a small fraction of the previous assemblages. The highest number of species ($N = 41$) (see Table 2) was identified in the ice sample collected on 5 June (the second sampling week).

The presence of the three known IP₂₅-producing taxa (*Haslea spicula*, *H. kjellmanii*, and *Pleurosigma stuxbergii* var.

TABLE 2 | List of diatom taxa encountered in sea-ice, sediment trap and surface sediment samples from the Young Sound fjord.

	Samples Young Sound			Culture
	ICE	TRAP	SED.	HBIs
CENTRIC DIATOMS				
<i>Actinocyclus curvatulus</i> Janisch		3	x	
<i>Bacterosira bathyomphala</i> spore	2		x	
<i>Chaetoceros</i> spp.				no
<i>Chaetoceros</i> spp. spore	1, 2, 3, 4, 5		x	
<i>Melosira arctica</i> Dickie	1, 2			
<i>Minidiscus proschkinae</i> (Makarova) Park & Lee	2			
<i>Porosira glacialis</i> (Grunow) Jørgensen	2			
<i>Skeletonema</i> cf. <i>costatum</i> (Greville) Cleve	2			
<i>Thalassiosira antarctica</i> var. <i>borealis</i> Fryxell, Doucette & Hubbard	2		x	
<i>T. antarctica</i> var. <i>borealis</i> spore		1, 2, 3	x	
<i>T. bulbosa</i> Syvertsen	2			
<i>T. gravida</i> Cleve	2			
<i>T. hyalina</i> (Grunow) Gran		3	x	
<i>T. hyperborea</i> (Grunow) Hasle	1, 2, 3, 4, 5			
<i>T. nordenskiöldii</i> Cleve		2, 3	x	no
<i>T. oceanica</i> Hasle	1			
<i>T. pacifica</i> Grunow & Angst		2		
<i>Thalassiosira</i> spp.	1, 2, 3	1, 3	x	no
PENNATE DIATOMS				
<i>Amphora</i> spp.		1	x	
<i>Bacillaria socialis</i> (Gregory) Ralfs		1		
<i>Biremis solitaria</i> (Cleve) Witkowski, Lange-Bertalot & Metzeltin	1, 2, 4			
<i>Biremis</i> spp.		1		
<i>Cocconeis costata</i> Gregory		1, 3	x	
<i>C. peltooides</i> Hustedt		1		
<i>C. scutellum</i> Ehrenberg		1, 2, 3	x	
<i>Cylindrotheca closterium</i> (Ehrenberg) Reimann & Lewin	2			
<i>Diploneis didyma</i> (Ehrenberg) Ehrenberg		1		
<i>D. litoralis</i> var. <i>clathrata</i> (Østrup) Cleve	2, 3, 4, 5	2		
<i>D. nitescens</i> (Gregory) Cleve		1		
<i>D. subcincta</i> (A. Schmidt) Cleve		1		
<i>Entomoneis kjellmanii</i> (Cleve) Poulin & Cardinal	1, 2			no
<i>E. pseudoduplex</i> Osada & Kobayasi	2			
<i>Entomoneis</i> sp.1	2			
<i>Fallacia clepsidroides</i> Witkowski		1		
<i>Fossula arctica</i> Hasle, Syvertsen & von Quillfeldt	1, 2, 3, 4, 5	1, 2, 3	x	
<i>Fragilaria</i> cf. <i>barbararum</i> Witkowski, Metzeltin & Lange-Bertalot	1, 2, 4, 5	1, 2, 3	x	
<i>Fragilaria</i> spp.		1, 2		
<i>Fragilariopsis cylindrus</i> (Grunow ex Cleve) Frenguelli	1, 2, 5	2, 3	x	
<i>F. oceanica</i> (Cleve) Hasle	1, 2, 3, 4	1, 2, 3	x	no
<i>F. reginae-jahniae</i> Witkowski, Lange-Bertalot & Metzeltin		2, 3	x	
<i>F. pseudonana</i> (Hasle) Hasle		2, 3		
<i>Grammatophora arcuata</i> Ehrenberg		1		
<i>Gyrosigma</i> spp.		1		
<i>Haslea crucigeroides</i> (Hustedt) Simonsen	2, 5			C25:3, C25:4
* <i>H. kjellmanii</i> (Cleve) Simonsen	3, 4			
* <i>H. spicula</i> (Hichie) Bukhtiyarova	1, 2, 3, 4, 5			IP ₂₅

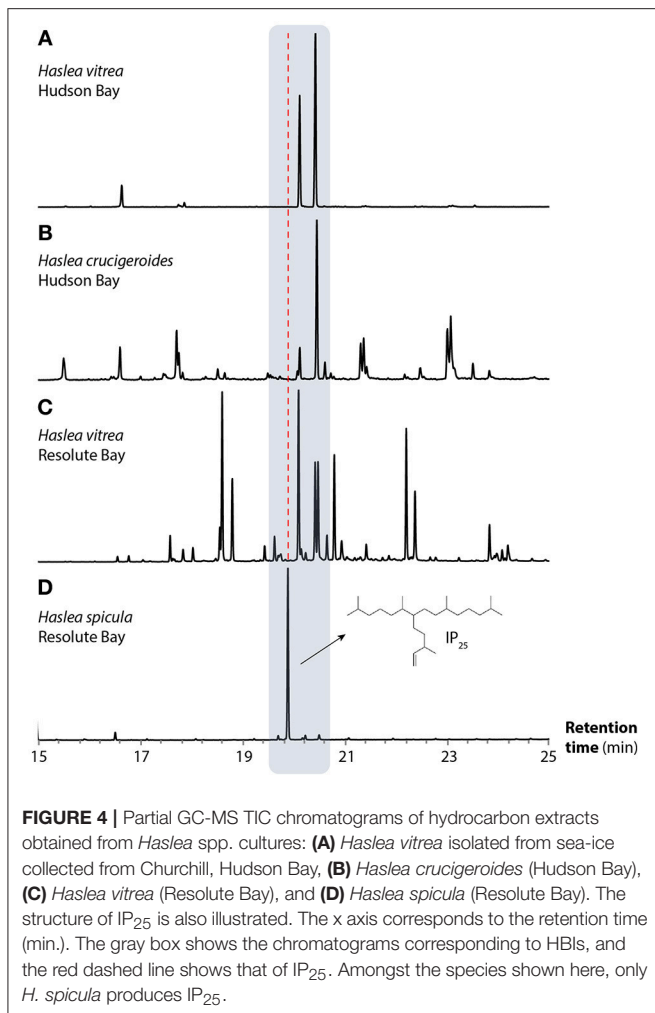
(Continued)

TABLE 2 | Continued

	Samples Young Sound			Culture
	ICE	TRAP	SED.	HBI
<i>H. vitrea</i> (Cleve) Simonsen	4			C25:3, C25:4
<i>Haslea</i> sp. 1	2			
<i>Lyrella spectabilis</i> (Gregory) Mann		1		
<i>Navicula directa</i> (W. Smith) Ralfs	1, 2	2		
<i>N. gelida</i> Grunow	3			
<i>N. kariana</i> var. <i>frigida</i> (Grunow) Cleve	1, 2, 4			
<i>N. lineola</i> Grunow	1, 2, 3, 4			
<i>N. lineola</i> var. <i>perlepida</i> (Grunow) Cleve	2, 3, 4			
<i>N. cf. oestrupii</i> Cleve	1, 3, 4			
<i>N. pellucidula</i> Hustedt	1, 2, 3, 4			
<i>N. transitans</i> Cleve	2, 4	2		
<i>N. vanhoeffenii</i> Gran	1, 2, 3, 4, 5	1		no
<i>N. veneta</i> Kützing	2			
<i>Navicula</i> spp.	1, 2, 3, 4, 5	1, 2, 3	x	no
<i>Nitzschia angularis</i> W. Smith	1, 4, 5			
<i>N. frigida</i> Grunow	1, 2, 3, 4, 5			no
<i>N. gelida</i> Cleve & Grunow	2, 3, 4			
<i>N. neofrigida</i> Medlin	1, 4, 5			
<i>Nitzschia</i> spp.	1, 2, 3, 4, 5	1, 3		no
<i>Opephora marina</i> (Gregory) Petit			x	
<i>Pauliella taeniata</i> (Grunow) Round & Basson	1, 2	3	x	no
<i>Pinnularia quadratarea</i> var. <i>constricta</i> (Østrup) Gran	2			
<i>P. quadratarea</i> var. <i>minor</i> (Grunow) Cleve	1, 4	2		
<i>Pinnularia</i> spp.	1	3		
<i>Planothidium delicatulum</i> -group		1, 3	x	
<i>Planothidium lemmermannii</i> (Hustedt) Morales		2		
* <i>Pleurosigma stuxbergii</i> var. <i>rhomboides</i> (Cleve) Cleve	1			
<i>Pleurosigma</i> spp.	1	1		no
<i>Psammodictyon roridum</i> (Giffen) Mann		1		
<i>Pseudofallacia tenera</i> (Hustedt) Liu, Kociolek & Wang		1		
<i>Pseudogomphonema septentrionale</i> (Østrup) Medlin	1			
<i>Pseudo-nitzschia seriata</i> (Cleve) H. Peragallo		2, 3		
<i>Rhoicosphenia marina</i> (Kützing) M. Schmidt		1		
<i>Stauroneis radissonii</i> Poulin & Cardinal	1, 2, 3, 4, 5			
<i>Stauroneis</i> sp.1	4			
<i>Stauroneis</i> spp.		1, 3		
<i>Stauronella arctica</i> (Hustedt) Lange-Bertalot	1, 2, 3, 4, 5	2		
<i>S. cf. decipiens</i> (Hustedt) Lange-Bertalot	2			
<i>Stenoneis wojtek-kowalskii</i> Witkowski, Lange-Bertalot & Metzeltin	1, 4, 5			
<i>Stenoneis</i> spp.	1			
<i>Tabularia tabulata</i> (C. Agardh) Snoeijis		1, 2	x	
<i>Thalassionema nitzschioides</i> (Grunow) Mereschkowsky		1		
<i>Trachyneis aspera</i> (Ehrenberg) Cleve		1		
<i>Thalassiothrix longissima</i> Cleve & Grunow		1		
<i>Ulnaria ulna</i> (Nitzsch) Compère		1		

The numbers correspond to the sea-ice or sediment trap samples in which they were found (refer to **Table 1**).

The x is used to mark the presence of the different taxa in the surface sediment sample. Typical sympagic taxa for which the HBI content was analyzed in the culture experiment are identified. The * indicates the IP₂₅-producing species according to Brown et al. (2014).



rhomboides) was validated through SEM observation. *Haslea crucigeroides*, which, like *H. vitrea* produces HBIs but not IP₂₅, was also observed (Table 1). The overall relative abundance of the three IP₂₅-producing taxa remained rather low over the five sampling weeks, with values ranging from 0.3 to 1.3%. This translated into total concentrations rising from 0.21 to 9.66 valves mL⁻¹. In line with these low numbers, measured concentrations of the lipid biomarker IP₂₅ were rather low during the entire sampling interval (from 0.4 to 0.7 pg mL⁻¹, Table 1). The concentrations of IP₂₅ and abundance of IP₂₅-producing species followed distinct trends over time (Figure 3).

Trap and Seafloor Sediments

The sediment trap collected particles during the intervals preceding (i) and during/following (ii) the seasonal ice melt:

(i) 24 April to 3 June 2014

A total of 33 taxa were identified (Supplementary Material). This assemblage was largely dominated by pennate diatom taxa including *Cocconeis* spp. (40%) and *Navicula* spp. (7%). The resting spores of both *Chaetoceros* spp. and *Thalassiosira antarctica* var. *borealis*

contributed to 7 and 4% of the assemblage, respectively (Figure 5). Furthermore, although *T. hyperborea* and *Nitzschia* spp. were important contributors to the ice assemblages, they were virtually absent from the sediment trap sample. The high abundance of benthic diatoms of the genus *Cocconeis* Ehrenberg in the sediment trap and its low abundance in the above sea-ice communities was likely due to events of resuspension of seafloor sediments.

(ii) 1 July to 4 August 2014; and 15 July to 4 August 2015

Both assemblages had a total of 20 taxa (Supplementary Material). Total centric diatoms, with important contributions of *Chaetoceros* spp. (vegetative cells and resting spores) and *Thalassiosira antarctica* var. *borealis* (resting spores), represented 36 and 61% of the assemblages in 2014 and 2015, respectively (Figure 5). The species *Fossula arctica* (23 and 14%), *Fragilariopsis oceanica* (20 and 11%), *F. cylindrus* (9 and 5%), and *F. reginae-jahniae* (5 and 2%) were also significant contributors to the assemblages.

None of the IP₂₅-producing diatom taxa were observed in any of the sediment trap samples analyzed.

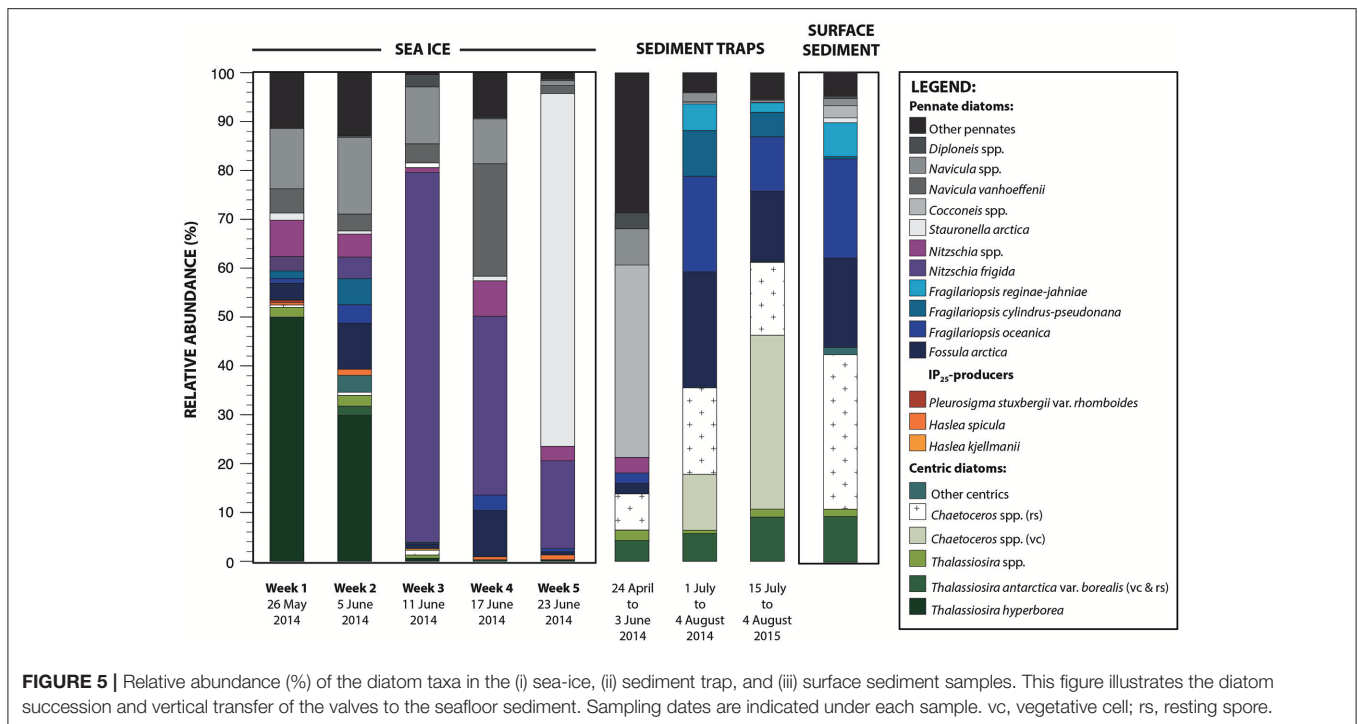
In the seafloor sediment sample, a total of 21 taxa belonging to 14 genera were identified (Supplementary Material). Resting spores of *Chaetoceros* spp. dominated the assemblage (32%). Other important taxa included *Fragilariopsis oceanica* (20%), *Fossula arctica* (18%), *Thalassiosira antarctica* var. *borealis* (resting spores) (9%), and *Fragilariopsis reginae-jahniae* (7%) (Figure 5). Neither IP₂₅-producing diatom taxa, nor *Nitzschia* spp. were recovered from the surface sediment sample. *Navicula* spp. represented ca. 2% of this assemblage.

The sedimentary IP₂₅ content was 20.69 ng g⁻¹ dry sediment or 1.56 μg g⁻¹ TOC (data from Ribeiro et al., 2017).

DISCUSSION

Seasonality of the Diatom Flora

The sea-ice algal assemblages were marked by rapid compositional shifts, with an initial dominance, and with low absolute concentrations, of the centric diatom *Thalassiosira hyperborea*. This species was also reported in sea-ice from other Arctic regions influenced by river discharge (Hasle and Lange, 1989). At our study site, its relative abundance decreased promptly, and this species was not identified in the sea-ice samples from the subsequent sampling weeks. It is therefore possible that these cells became entrapped in the sea-ice when it formed during the preceding autumn. The most steady and significant contributors to the sea-ice communities were taxa belonging to the pennate genera *Nitzschia* Hassall and *Navicula* Bory. The latter were further characterized by high species diversity (Table 2). In this respect, the assemblages from the studied fjord are comparable to those from other seasonally sea-ice covered Arctic regions where these two genera, and especially *Nitzschia frigida*, are typically found in the sea-ice (e.g., Medlin and Hasle, 1990; Syvertsen, 1991; Rózanska et al., 2009; Poulin et al., 2011; Leu et al., 2015; Olsen et al., 2017). The high relative abundance of the pennate *Stauronella arctica* during the last sampling week was however surprising since this species



has, to our knowledge, never been reported to dominate sea-ice assemblages in the Arctic.

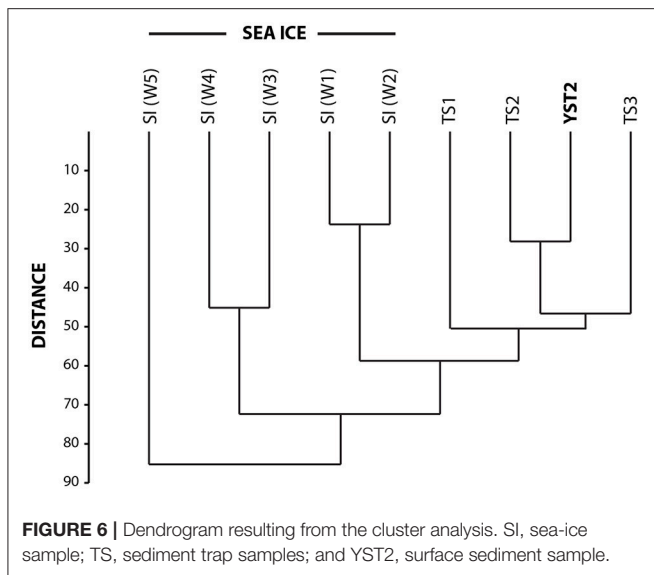
Although *Fossula arctica*, *Fragilariopsis cylindrus*, and *F. oceanica* contributed to the sea-ice flora, their highest relative abundances were found in the trap and surface sediment samples. This suggests that, in this study area, their growth was likely favored during the final stage of sea-ice retreat, and in the surface-water environment resulting from melt (e.g., cold and low-salinity). This is coherent with observations from other sea-ice covered regions that have associated these species with the pelagic vernal bloom (e.g., Kang and Fryxell, 1992; Hasle et al., 1996; von Quillfeldt, 2000, 2004). By contrast to the *Fragilariopsis* species mentioned above, *F. reginae-jahniae* was only observed in the trap and surface sediment samples, suggesting that it colonizes the sea-ice or surface-waters later in the season. The high abundances of both vegetative cells and resting spores of *Chaetoceros* Ehrenberg in the two July sediment traps suggest that more open conditions are required for these to thrive. Blooms of colonial centric *Chaetoceros* spp. have been reported to occur along the marginal ice zone (e.g., Wassmann et al., 1999), but are often found at highest concentrations later in the season (e.g., von Quillfeldt, 2000; Krawczyk et al., 2014). The production of resting spores can occur massively over a short period of time (e.g., Rembauville et al., 2018), as part of a survival strategy that includes a benthic reservoir of resistant cells that can function as inoculum for the next growing season. In the North Water polynya, *Chaetoceros* sp. produce large quantities of fast sinking resting spores as a response to nutrient depletion, allowing the population to be sustained for an extended period of time (Booth et al., 2002). Overall, observations made here are in line with those reported by Krawczyk et al. (2015), showing alternating

dominance of *Fragilariopsis* spp. and *Chaetoceros* spp. in the pelagic protist assemblages of Young Sound, in July/August of 2010–2012 and 2009–2011, respectively.

Vertical Export of IP₂₅ and Diatom Valves

Several diatom genera identified from the sea-ice, notably *Nitzschia*, *Haslea* Simonsen, and *Navicula*, were only sporadically observed in the trap and surface sediment samples, and most of the time as fragments. From our dataset, it is difficult to determine whether their absence or low representation in the sediments was primarily due to degradation during vertical sinking or caused by a “dilution effect” due to the dominance of the main spring blooming species. Our observations are however consistent with studies from other Arctic regions where these are generally rare or absent (e.g., Moros et al., 2006; Sha et al., 2014; Krawczyk et al., 2017). Similarly, the weakly silicified vegetative cells of *Chaetoceros* spp., that were important contributors to the phytoplankton community as illustrated by their high abundance in the second set of trap samples, were not reported from the surface sediment sample. Compared to the vegetative cells, the resting spores of *Chaetoceros* can be 3–4 times more silicified (Rynearson et al., 2013), allowing them to sink more rapidly toward the seafloor. They have been proven to be more resistant to bacterial degradation (Kuwata and Takahashi, 1990) and remain intact after being digested by zooplankton (Kuwata and Tsuda, 2005). All of these factors favor their export to, and preservation in, the seafloor sediments.

All the diatom taxa that were identified from the surface sediments were also observed either in the sea-ice or sediment trap samples. Classical cluster analysis shows that the diatom assemblage from the surface sediment sample was most similar



to that of the sediment trap sample that covers the interval from 1 July to 4 August 2014, which represents the melt and post-melt diatom production (**Figure 6**). This is coherent with data from Rysgaard et al. (2001) showing that ice algae only contribute to a minor fraction (<1%) of the total pelagic primary production in the fjord.

Although the sedimentary IP₂₅ (20.69 ng g⁻¹ dry sediment or 1.56 μg g⁻¹ TOC) content was relatively low, i.e., up to 7 times lower than the values reported from other marine Arctic settings where sea-ice lasts throughout spring/summer (e.g., Müller et al., 2011; Xiao et al., 2015), it is comparable to the values reported from other regions influenced by river or meltwater runoff (e.g., Xiao et al., 2013; Limoges et al., 2018). The low IP₂₅ concentrations in the sediments are consistent with the low concentrations of IP₂₅-producing taxa found in the fjord's sea-ice. During the fourth and fifth week of sampling, while the total abundance of IP₂₅-producing species increased, IP₂₅ concentrations measured from sea-ice stabilized and decreased (**Figure 3**). The absence of a relationship between the concentrations of IP₂₅-producing species and the lipid IP₂₅ in the sea-ice samples may arise from (i) intra-specific differences in the production of IP₂₅ and subtle changes in the relative contribution of the different IP₂₅-producing species in sea-ice, and/or (ii) changes in the intracellular biosynthesis of IP₂₅ in response to environmental conditions (e.g., light intensity, salinity, temperature, nutrients, etc.). We note that Brown et al. (2014) measured relatively similar intracellular IP₂₅ concentration (ranging from ca. 0.6 to 3.8 pg cell⁻¹) for each of the IP₂₅-producing diatom taxa investigated. Here, the potential impact of those parameters other than sea-ice presence on the intracellular IP₂₅ biosynthesis cannot be excluded nor quantified individually, and we recognize that further studies would be needed to address this. Since the abundance of IP₂₅-producing species increases in parallel to a slight decrease in the salinity of the sea-ice bottom (**Figure 3**), our data do not indicate a

direct adverse impact of low-salinity on the abundance of IP₂₅-producing species, but neither rule out a potential effect of low-salinity on IP₂₅ synthesis.

Implications for Paleo-Environmental Studies

The main contributors to the surface sediment assemblage were resting spores of the centric diatom *Chaetoceros* and *Thalassiosira antarctica* var. *borealis*, and the pennate *Fossula arctica*, *Fragilariopsis oceanica*, and *F. reginae-jahniae*. All of these (except *F. reginae-jahniae*) were minor components of the sea-ice communities, but their peak abundances occurred during or following ice melt. Based on previous work (e.g., von Quillfeldt, 2000, 2001), the pennate *Fossula arctica*, and *Fragilariopsis oceanica*, as well as *Fragilariopsis cylindrus*, which have been frequently used as sea-ice indicator species in paleoceanographic studies, occur earlier in the spring and appear to reflect the cold and low surface salinity conditions of the marginal ice zone. *Thalassiosira antarctica* var. *borealis* and *Chaetoceros* spp. on the other hand generally bloom later in the season, when the cold and low-salinity surface layer is breaking up and the mixing layer is deeper. These successional characteristics of diatom communities are important to take into account when interpreting palaeo-records from Arctic regions.

The confirmed presence of three IP₂₅-producing species (*Haslea spicula*, *H. kjellmanii*, and *Pleurosigma stuxbergii* var. *rhomboides*) in the Young Sound together with the detection of IP₂₅ in the sea-ice samples is of critical importance because it provides direct evidence for *in-situ* production of IP₂₅ in this fjord, even though some additional advection of the biomarker from offshore waters cannot be excluded. The weak IP₂₅ sedimentary fingerprint does not appear to be the result of diagenetic processes during vertical transfer toward the sediment but is rather consistent with low overall diatom production and low abundance of IP₂₅-producing species in the fjord ice. In Young Sound, total sea-ice diatom concentrations increased from 21 to 985 valves mL⁻¹ (or ca. 11 to 493 cells mL⁻¹) over the five sampling weeks, which is markedly lower than what is reported from other Arctic regions. For example, Hsiao (1980) reported total diatom concentrations of up to ca. 40,000 cells mL⁻¹ in the bottom 10 cm of sea-ice cores collected in May 1972 from Husky Lakes (formerly known as Eskimo Lakes), Northwest Territories, Canada. Riedel et al. (2003) also reported concentrations of more than 100,000 cells mL⁻¹ in the bottom 3–5 cm of sea-ice cores collected in May 2001 from McDougall Sound, near Resolute Bay, Nunavut. We must note that these differences could be due, in part, to significant spatio-temporal variabilities in-ice biomass (e.g., Lange et al., 2017), and limited ice sampling here. The low production in Young Sound is also possibly related to the ecological needs of the different diatom species and environmental parameters, other than the simple presence of sea-ice (e.g., nutrient levels, light, temperature, salinity, etc.), that affect their growth and steer the assemblage composition. The relative abundance of IP₂₅-producing species (0.3 to 1.3% of sympagic assemblages) is at the low end of the range reported from a number of sites in

the Arctic by (Brown et al. (2014), their Table 3). This suggests that Young Sound is only marginally suitable for the growth of IP₂₅-producing species. Importantly, it has been shown that the bottom horizon of sea-ice (0–3 cm) is strongly affected by the properties of the under-ice surface-water (e.g., Reeburgh, 1984). Poulin et al. (1983) and Gosselin et al. (1986) suggested that lower under-ice salinity negatively influences the settlement efficiency of sympagic microalgal populations, through its role in shaping the microstructure of the ice. Such interplay between salinity, ice porosity, and sea-ice algal colonization was observed in coastal sea-ice, in the Gulf of Finland (Granskog et al., 2005). Although it might be challenging to mimic sea-ice conditions in the laboratory, carefully designed culture experiments are recommended to test the growth and IP₂₅ production of the source species under different environmental conditions. In particular, cultures under salinity conditions that are similar to those observed in fjords influenced by meltwater during spring/summer are needed.

In light of the observations made here, as well as in other studies documenting the modern distribution of IP₂₅ in sediments from areas influenced by freshwater (Xiao et al., 2013; Hörner et al., 2016; Ribeiro et al., 2017; Limoges et al., 2018), we recommend careful interpretation of paleo sea-ice records based on the sedimentary IP₂₅ signal in regions that are susceptible to significant inter-annual, but also longer-term changes in salinity. Lower salinities may influence the structural nature of sea-ice and its propensity to sustain algal growth, including IP₂₅-producing diatom species. As stated above, it is also plausible that low-salinity conditions, as well as other parameters (e.g., light intensity, nutrient levels) influence IP₂₅ synthesis and intracellular concentration in these species. To summarize, in fjords and coastal embayment regions, the presence of IP₂₅ may for now be regarded as a signal of presence of seasonal sea-ice, rather than a robust indicator of variability in sea-ice concentration. In all cases, multi-proxy approaches are preferred to allow for a more critical evaluation of the paleo-environmental signal derived from this biomarker.

CONCLUSIONS

The spring diatom succession was captured by the sea-ice and sediment trap samples. An important shift in the composition of the assemblages was recorded, with an early diatom colonization by the centric *Thalassiosira hyperborea*, which was rapidly replaced by pennate diatoms belonging to *Nitzschia* and *Navicula* species, and *Stauronella arctica*. *Fossula arctica*, other *Fragilariopsis*, *Thalassiosira antarctica* var. *borealis* spores, and *Chaetoceros* spp. (vegetative cells and resting spores) appeared to thrive in the melt and post-melt environment. The surface sediment diatom assemblages were dominated by the pennate

diatoms *Fragilariopsis oceanica*, *Fossula arctica*, *Fragilariopsis reginae-jahniae* and the resting spores of the centric diatoms *Thalassiosira antarctica* var. *borealis* and *Chaetoceros* spp. The paleo-environmental signal preserved by the diatom assemblages in the surface sediment therefore primarily reflected the melt and post-melt sea-surface conditions.

This study confirms the *in-situ* production of the sea-ice biomarker IP₂₅ in this fjord system and that *Haslea spicula* is one of the species responsible for the production of the sea-ice biomarker IP₂₅. *Haslea crucigeroides*, like *H. vitrea*, produced other HBIs (including triene) but not IP₂₅. Finally, while IP₂₅ is produced in seasonally sea-ice covered coastal environments with freshwater influence, it may not reflect variability in sea-ice concentrations. In the Young Sound, the growth of IP₂₅-producing diatom taxa, and possibly also their cellular IP₂₅ synthesis, appear to be affected by the physico-chemical conditions (e.g., light, salinity, nutrient levels) that prevail in the sea-ice microenvironment.

AUTHOR CONTRIBUTIONS

This study was conceptualized by SRi and designed by SRi, GM, KW, and AL. Sampling and *in-situ* measurements were done by N-XG, MS, and SRy. Preparations and analyses were done by KW, GM, ME, and AL. Interpretation of the results was done by SRi, KW, GM, MP, and AL. The manuscript was written by AL with intellectual additions, discussions and revisions by all other co-authors (GM, KW, MP, ME, MH, N-XG, MS, SRy, and SRi). All authors provided their approval for the publication of this manuscript.

ACKNOWLEDGMENTS

This study received financial support from the Villum Foundation, Denmark (grant VKR023454 to SRi). Fieldwork was funded by the Arctic Research Center at Aarhus University. We are grateful to Tage Dalsgaard for help in the laboratory. AL and GM received financial support from NSERC-discovery grant (grants RGPIN-2018-03984 & RGPIN-2016-05945). MH and KW acknowledge funding from the Academy of Finland (grants 296895 and 307282). SR was funded by the Canada Excellence Research Chair Program. Finally, we acknowledge the constructive comments of two reviewers and handling editor, Dr. Flores.

SUPPLEMENTARY MATERIAL

The Supplementary Material for this article can be found online at: <https://www.frontiersin.org/articles/10.3389/feart.2018.00226/full#supplementary-material>

REFERENCES

Andrews, J. T., Belt, S. T., Olafsdottir, S., Massé, G., and Vare, L. L. (2009). Sea ice and climate variability for NW Iceland/Denmark Strait over the last 2000 cal yr BP. *Holocene* 19, 775–784. doi: 10.1177/0959683609105302

Battarbee, R. W., Jones, V. J., Flower, R. J., Cameron, N. G., Bennion, H., Carvalho, L., et al. (2001). "Tracking environmental change using lake sediments," in *Terrestrial, Algal, and Siliceous Indicators*, Vol. 3, eds J. Diatoms and P. Smol Dordrecht (Netherlands: Kluwer), 155–202. doi: 10.1007/0-306-47668-1_8

- Belt, S. T., Massé, G., Rowland, S. J., Poulin, M., Michel, C., and Leblanc, B. (2007). A novel chemical fossil of palaeo sea ice: IP₂₅. *Org. Geochem.* 38, 16–27. doi: 10.1016/j.orggeochem.2006.09.013
- Belt, S. T., and Müller, J. (2013). The Arctic sea ice biomarker IP₂₅: a review of current understanding, recommendations for future research and applications in palaeo sea ice reconstructions. *Quat. Sci. Rev.* 79, 9–25. doi: 10.1016/j.quascirev.2012.12.001
- Belt, S. T., Vare, L., Massé, G., Manners, H. R., Price, J. C., MacLachlan, S. E., et al. (2010). Striking similarities in temporal changes to spring sea ice occurrence across the central Canadian Arctic Archipelago over the last 7000 years. *Quat. Sci. Rev.* 29, 3489–3504. doi: 10.1016/j.quascirev.2010.06.041
- Bendtsen, J., Mortensen, J., Lennert, K., Ehn, J. K., Boone, W., Galindo, V., et al. (2017). Sea ice breakup and marine melt of a retreating tidewater outlet glacier in northeast Greenland (81°N). *Sci. Rep.* 7:4941. doi: 10.1038/s41598-017-05089-3
- Boone, W., Rysgaard, S., Carlson, D. F., Meire, L., Kirillov, S., Mortensen, J., et al. (2018). Coastal freshening prevents fjord bottom water renewal in Northeast Greenland: a mooring study from 2003 to 2015. *Geophys. Res. Lett.* 45, 2726–2733. doi: 10.1002/2017GL076591
- Booth, B. C., Larouche, P., Bélanger, S., Klein, B., Amiel, D., and Mei, Z. P. (2002). Dynamics of *Chaetoceros socialis* blooms in the North water. *Deep-Sea Res. II* 49, 5003–5025. doi: 10.1016/S0967-0645(02)00175-3
- Brown, T. A., Belt, S., Philippe, B., Mundy, C. J., Massé, G., Poulin, M., et al. (2011). Temporal and vertical variations of lipid biomarkers during a bottom ice diatom bloom in the Canadian Beaufort Sea: further evidence for the use of the IP₂₅ biomarker as a proxy for spring Arctic sea ice. *Polar. Biol.* 34, 1857–1868. doi: 10.1007/s00300-010-0942-5
- Brown, T. A., Belt, S. T., Tatarek, A., and Mundy, C. J. (2014). Source identification of the Arctic sea ice proxy IP₂₅. *Nat. Commun.* 5:4197. doi: 10.1038/ncomms5197
- Cabedo-Sanz, P., and Belt, S. T. (2016). Seasonal sea ice variability in eastern Fram Strait over the last 2,000 years. *Arktos* 2:22. doi: 10.1007/s41063-016-0023-2
- Curry, J. A., Schramm, J. L., and Ebert, E. E. (1995). Sea ice-albedo climate feedback mechanism. *J. Clim.* 8, 240–247. doi: 10.1175/1520-0442(1995)008<0240:SIACFM>2.0.CO;2
- de Vernal, A., Gersonde, R., Goosse, H., Seidenkrantz, M. S., and Wolff, E. W. (2013). Sea ice in the paleoclimate system: the challenge of reconstructing sea ice from proxies – An introduction. *Quat. Sci. Rev.* 79, 1–8. doi: 10.1016/j.quascirev.2013.08.009
- Gosselin, M., Legendre, L., Theriault, J. C., Demers, S., and Rochet, M. (1986). Physical control of the horizontal patchiness of sea-ice microalgae. *Mar. Ecol. Progr. Ser.* 29, 289–298. doi: 10.3354/meps029289
- Granskog, M. A., Kaartokallio, H., Thomas, D. N., and Kuosa, H. (2005). Influence of freshwater inflow on the inorganic nutrient and dissolved organic matter within coastal sea ice and underlying waters in the Gulf of Finland (Baltic Sea). *Estuar. Coast. Shelf Sci.* 65, 109–122.
- Hammer, Ø., Harper, D. A. T., and Ryan, P. D. (2001). *PAST: Paleontological Statistics Software Package for Education*. Oslo.
- Hasle, G. R., and Lange, C. B. (1989). Freshwater and brackish water *Thalassiosira* (*Bacillariophyceae*): taxa with tangentially undulated valves. *Phycologia* 28, 120–135. doi: 10.2216/i0031-8884-28-1-120.1
- Hasle, G. R., Syvertsen, E. E., and von Quillfeldt, C. H. (1996). *Fossula arctica* gen nov., spec. nov., a marine Arctic araphid diatom. *Diatom Res.* 11, 261–272. doi: 10.1080/0269249X.1996.9705383
- Hörner, T., Stein, R., Fahl, K., and Birgel, D. (2016). Post-glacial variability of sea ice cover, river run-off and biological production in the western Laptev Sea (Arctic Ocean)—a high-resolution biomarker study. *Quat. Sci. Rev.* 143, 133–149. doi: 10.1016/j.quascirev.2016.04.011
- Hsiao, S. I. C. (1980). Quantitative composition, distribution, community structure and standing stock of sea ice microalgae in the Canadian Arctic. *Arctic* 33, 768–793. doi: 10.14430/arctic2595
- Hustedt, F. (1961). “Die Kieselalgen Deutschlands, Österreichs und der Schweiz,” in *Kryptogamenflora von Deutschland, Österreich und der Schweiz, Band 7, Teil 3, Lief. 1*, ed. L. Rabenhorsts (Leipzig: Akademische Verlagsgesellschaft), 1–160.
- Jahn, A., and Holland, M. M. (2013). Implications of Arctic sea ice changes for North Atlantic deep convection and the meridional overturning circulation in CCSM4-CMIP5 simulations. *Geophys. Res. Lett.* 40, 1206–1211. doi: 10.1002/grl.50183
- Jensen, L. M., Christensen, T. R., and Schmidt, N. M. (2014). *Zackenbergs Ecological Research Operations, 19th Annual Report 2013*. Roskilde: DCE-Danish Centre for Environment and Energy, Aarhus University. 130.
- Kang, S. H., and Fryxell, G. A. (1992). *Fragilariopsis cylindrus* (Grunow) Krieger – The most abundant diatom in water column assemblages of Antarctic marginal ice-edge zones. *Polar Biol.* 12, 609–627. doi: 10.1007/BF00236984
- Krawczyk, D. W., Arendt, K. E., Juul-Pedersen, T., Sejr, M. K., Blicher, M. E., and Jakobsen, H. H. (2015). Spatial and temporal distribution of planktonic protists in the East Greenland fjord and offshore waters. *Mar. Ecol. Progr. Ser.* 538, 99–116. doi: 10.3354/meps11439
- Krawczyk, D. W., Witkowski, A., Moros, M., Lloyd, J. M., Høyer, J. L., Miettinen, A., et al. (2017). Quantitative reconstruction of Holocene sea ice and sea surface temperature off West Greenland from the first regional diatom data set. *Paleoceanography* 32, 18–40. doi: 10.1002/2016PA003003
- Krawczyk, D. W., Witkowski, A., Waniek, J. J., Wroniecki, M., and Harff, J. (2014). Description of diatoms from the Southwest to West Greenland coastal and open marine waters. *Polar Biol.* 37, 1589–1606. doi: 10.1007/s00300-014-1546-2
- Kroon, A., Abermann, J., Bendixen, M., Lund, M., Sigsgaard, C., Skov, K., et al. (2017). Deltas, freshwater discharge, and waves along the Young Sound, NE Greenland. *Ambio* 16, 132–145. doi: 10.1007/s13280-016-0869-3
- Kuwata, A., and Takahashi, M. (1990). Life-form population responses of a marine planktonic diatom, *Chaetoceros pseudocurvisetus*, to oligotrophication in regionally upwelled water. *Mar. Biol.* 107, 503–512. doi: 10.1007/BF01313435
- Kuwata, A., and Tsuda, A. (2005). Selection and viability after ingestion of vegetative cells, resting spores and resting cells of the marine diatom, *Chaetoceros pseudocurvisetus*, by two copepods. *J. Exp. Mar. Biol. Ecol.* 322, 143–151. doi: 10.1016/j.jembe.2005.02.013
- Lange, B. A., Katlein, C., Castellani, G., Fernández-Méndez, M., Nicolaus, M., Peeken, I., et al. (2017). Characterizing spatial variability of ice aggl chlorophyll a and net primary production between sea ice habitats using horizontal profiling platforms. *Front. Mar. Sci.* 4:349. doi: 10.3389/fmars.2017.00349
- Leu, E., Mundy, C. J., Assmy, P., Campbell, K., Gabrielsen, T. M., Gosselin, M., et al. (2015). Arctic spring awakening – steering principles behind the phenology of vernal ice blooms. *Prog. Oceanogr.* 139, 151–170. doi: 10.1016/j.pcean.2015.07.012
- Limoges, A., Ribeiro, S., Weckström, K., Heikkilä, M., Zamelczyk, K., Andersen, T. J., et al. (2018). Linking the modern distribution of biogenic proxies in High Arctic Greenland shelf sediments to sea ice, primary production, and Arctic-Atlantic inflow. *J. Geophys. Res.* 123, 760–786. doi: 10.1002/2017JG003840
- Lundholm, N., Daugbjerg, N., and Moestrup, Ø. (2002). Phylogeny of the Bacillariaceae with emphasis on the genus *Pseudo-nitzschia* (*Bacillariophyceae*) based on partial LSU rDNA. *Eur. J. Phycol.* 37, 115–134. doi: 10.1017/S096702620100347X
- Massé, G., Rowland, S. J., Sicre, M. A., Jacob, J., Jansen, E., and Belt, S. T. (2008). Abrupt climate changes for Iceland during the last millennium: evidence from high resolution sea ice reconstructions. *Earth Planet. Sci. Lett.* 269, 565–569. doi: 10.1016/j.epsl.2008.03.017
- Medlin, L. K., and Hasle, G. R. (1990). Some *Nitzschia* and related diatom species from fast ice samples in the Arctic and Antarctic. *Polar Biol.* 10, 451–479. doi: 10.1007/BF00233693
- Mernild, S. H., Sigsgaard, C., Rasch, M., Hasholt, B., Hansen, B. U., Stjernholm, M., et al. (2007). “Climate, river discharge and suspended sediment transport in the Zackenberg River drainage basin and Young Sound/Tyrolerfjord, Northeast Greenland, 1995–2003,” in *Carbon Cycling in Arctic marine ecosystems. Case study Young Sound*, eds S. Rysgaard, R. N. Glud, and T. M. Roberts (Leine: Meddr. Grøland), 24–43.
- Moros, M., Jensen, K. G., and Kuijpers, A. (2006). Mid- to late-Holocene hydrological and climatic variability in Disko Bugt, central West Greenland. *Holocene* 16, 357–367. doi: 10.1191/0959683606hl933rp
- Müller, J., Wagner, A., Fahl, K., Stein, R., Prange, M., and Lohmann, G. (2011). Towards quantitative sea ice reconstructions in the northern North Atlantic: a combined biomarker and numerical modelling approach. *Earth Planet. Sci. Lett.* 306, 137–148. doi: 10.1016/j.epsl.2011.04.011
- Müller, J., Werner, K., Stein, R., Fahl, K., Moros, M., and Jansen, E. (2012). Holocene cooling culminates in sea ice oscillations in Fram Strait. *Quat. Sci. Rev.* 47, 1–14. doi: 10.1016/j.quascirev.2012.04.024
- Olsen, L. S., Laney, S. R., Duarte, P., Kauko, H. M., Fernandez-Mendez, M., Mundy, C. J., et al. (2017). The seeding of ice algal blooms in Arctic pack ice:

- the multiyear ice seed repository hypothesis. *J. Geophys. Res.* 122, 1529–1548. doi: 10.1002/2016JG003668
- Polyak, L., Alley, R. B., Andrews, J. T., Brigham-Grette, J., Cronin, T. M., Darby, D. A., et al. (2010). History of sea ice in the Arctic. *Quat. Sci. Rev.* 29, 1757–1778. doi: 10.1016/j.quascirev.2010.02.010
- Poulin, M., Cardinal, A., and Legendre, L. (1983). Réponse d'une communauté de diatomées de glace à un gradient de salinité (baie d'Hudson). *Mar. Biol.* 76, 191–202.
- Poulin, M., Daugbjerg, N., Gradinger, R., Ilyash, L., Ratkova, T., and von Quillfeldt, C. (2011). The pan-Arctic biodiversity of marine pelagic and sea-ice unicellular eukaryotes: a first-attempt assessment. *Mar. Biodiv.* 41, 13–28. doi: 10.1007/s12526-010-0058-8
- Reeburgh, W. S. (1984). Fluxes associated with brine motion in growing sea ice. *Polar Biol.* 3, 29–33.
- Rembauville, M., Blain, S., Manno, C., Tarling, G., Thompson, A., Wolf, G., et al. (2018). The role of diatom resting spores in pelagic–benthic coupling in the Southern Ocean. *Biogeosciences* 15, 3071–3084. doi: 10.5194/bg-15-3071-2018
- Ribeiro, S., Sejr, M. K., Limoges, A., Heikkilä, M., Andersen, T. J., Tallberg, P., et al. (2017). Sea ice and primary production proxies in surface sediments from a High Arctic Greenland fjord: spatial distribution and implications for palaeoenvironmental studies. *Ambio* 26 (Suppl. 1), 106–118. doi: 10.1007/s13280-016-0894-2
- Riedel, A., Michel, C., Poulin, M., and Lessard, S. (2003). Taxonomy and abundance of microalgae and protists at a first-year sea ice station near Resolute Bay, Nunavut, Spring to early Summer 2001. *Can. Data Rep. Hydrogr. Ocean Sci.* 159, 1–53.
- Rontani, J. F., Belt, S. T., and Amiraux, R. (2018). Biotic and abiotic degradation of the sea ice diatom biomarker IP₂₅ and selected algal sterols in near-surface Arctic sediments. *Org. Geochem.* 118, 73–88. doi: 10.1016/j.orggeochem.2018.01.003
- Rózanska, M., Gosselin, M., Poulin, M., Wiktor, J. M., and Michel, C. (2009). Influence of environmental factors on the development of bottom ice protist communities during the winter-spring transition. *Mar. Ecol. Prog. Ser.* 386, 43–59. doi: 10.3354/meps08092
- Ryneron, T. A., Richardson, K., Lampitt, R. S., Sieracki, M. E., Poulton, A. J., Lyngsgaard, M. M., et al. (2013). Major contribution of diatom resting spores to vertical flux in the sub-polar North Atlantic. *Deep-Sea Res. I* 82, 60–71. doi: 10.1016/j.dsr.2013.07.013
- Rysgaard, S., and Glud, R. N. (2007). Carbon cycling in Arctic marine ecosystems: case study - young sound. *Meddelelser om Grønland. Bioscience* 58, 176–191.
- Rysgaard, S., Kühl, M., Glud, R. N., and Hansen, J. W. (2001). Biomass, production and horizontal patchiness of sea ice algae in a high-Arctic fjord (Young Sound, NE Greenland). *Mar. Ecol. Prog. Ser.* 223, 15–26. doi: 10.3354/meps223015
- Rysgaard, S., Nielsen, T. G., and Hansen, B. W. (1999). Seasonal variation in nutrients, pelagic primary production and grazing in a high-Arctic coastal marine ecosystem, Young Sound, Northeast Greenland. *Mar. Ecol. Prog. Ser.* 179, 13–25. doi: 10.3354/meps179013
- Rysgaard, S., Sejr, M. K., Frandsen, E. R., Frederiksen, M., Arendt, K., and Mikkelsen, D. M. (2009). *The Zackenberg Marine Monitoring Programme: Sampling Manual for the Annual Summer Field Campaign*. Greenland Institute of Natural Resources and National Environmental Research Institute, Denmark.
- Rysgaard, S., Vang, T., Stjernholm, M., Rasmussen, B., Windelin, A., and Kiilsholm, S. (2003). Physical conditions, carbon transport, and climate change impacts in a Northeast Greenland Fjord. *Arct. Antarct. Alp. Res.* 35, 301–312. doi: 10.1657/1523-0430(2003)035[0301:PCCTAC]2.0.CO;2
- Sejr, M. K., Stedmon, C. A., Bendtsen, J., Abermann, J., Juul-Pedersen, T., Mortensen, J., et al. (2017). Evidence of local and regional freshening of Northeast Greenland coastal waters. *Sci. Rep.* 7:13183. doi: 10.1038/s41598-017-10610-9
- Serreze, M. C., and Barry, R. G. (2011). Processes and impacts of Arctic amplification: a research synthesis. *Glob. Planet. Change* 77, 85–96. doi: 10.1016/j.gloplacha.2011.03.004
- Sha, L., Jiang, H., Seidenkrantz, M. S., Knudsen, K. L., Olsen, J., Kuijpers, A., et al. (2014). A diatom-based sea-ice reconstruction for the Vaigat Strait (Disko Bugt, West Greenland) over the last 5000 yr. *Palaeogeogr. Palaeoclimatol. Palaeoecol.* 403, 66–79. doi: 10.1016/j.palaeo.2014.03.028
- Snoeijs, P. (1993). *Intercalibration and Distribution of Diatom Species in the Baltic Sea*, Vol. 1, Uppsala: Opulus Press; Baltic Marine Biologist Publication 16a.
- Snoeijs, P., and Balashova, N. (1998). *Intercalibration and Distribution of Diatom Species in the Baltic Sea*, Vol. 5, Uppsala: Opulus Press; Baltic Marine Biologist Publication 16e.
- Snoeijs, P., and Kasperoviciene, J. (1996). *Intercalibration and Distribution of Diatom Species in the Baltic Sea*, Vol. 4, Uppsala: Opulus Press; Baltic Marine Biologist Publication 16d.
- Snoeijs, P., and Potapova, M. (1995). *Intercalibration and Distribution of Diatom Species in the Baltic Sea*, Vol. 3, Uppsala: Opulus Press; Baltic Marine Biologist Publication 16c.
- Snoeijs, P., and Vilbaste, S. (1994). *Intercalibration and Distribution of Diatom Species in the Baltic Sea*. Vol. 2, Uppsala: Opulus Press; Baltic Marine Biologist Publication 16b.
- Syvrtsen, E. E. (1991). Ice algae in the Barents Sea: types of assemblages, origin fate and role in the ice-edge phytoplankton bloom. *Polar Res.* 10, 277–288. doi: 10.3402/polar.v10i1.6746
- Tomas, R. A., Deser, C., and Sun, L. (2016). The role of ocean heat transport in the global climate response to projected Arctic sea ice loss. *J. Clim.* 29, 6841–6859. doi: 10.1175/JCLI-D-15-0651.1
- Vare, L. L., Massé, G., Gregory, T. R., Smart, C. W., and Belt, S. T. (2009). Sea ice variations in the central Canadian Arctic Archipelago during the Holocene. *Quat. Sci. Rev.* 28, 1354–1366. doi: 10.1016/j.quascirev.2009.01.013
- von Quillfeldt, C. H. (2000). Common diatom species in Arctic spring blooms: their distribution and abundance. *Bot. Mar.* 43, 499–516. doi: 10.1515/BOT.2000.050
- von Quillfeldt, C. H. (2001). Identification of some easily confused common diatom species in Arctic spring blooms. *Bot. Mar.* 44, 375–389. doi: 10.1515/BOT.2001.048
- von Quillfeldt, C. H. (2004). The diatom *Fragilariopsis cylindrus* and its potential as an indicator species for cold water rather than for sea ice. *Vie et Milieu* 5, 137–143.
- Wassmann, P., Ratkova, T., Andreassen, I., Vernet, M., Pedersen, G., and Rey, F. (1999). Spring bloom development in the marginal ice zone and the central Barents Sea. *Mar. Ecol. Prog. Ser.* 20, 321–246. doi: 10.1046/j.1439-0485.1999.2034081.x
- Witkowski, A., Lange-Bertalot, H., and Metzeltin, D. (2000). Diatom flora of marine coasts. *I. Iconogr. Diatomol.* 7, 1–925.
- Xiao, X., Fahl, K., Müller, J., and Stein, R. (2015). Sea-ice distribution in the modern Arctic Ocean: biomarker records from trans-Arctic Ocean surface sediments. *Geochim. Cosmochim. Acta* 155, 16–29. doi: 10.1016/j.gca.2015.01.029
- Xiao, X., Fahl, K., and Stein, R. (2013). Biomarker distribution in surface sediments from the Kara and Laptev seas (Arctic Ocean): indicators for organic-carbon sources and sea-ice coverage. *Quat. Sci. Rev.* 79, 40–52. doi: 10.1016/j.quascirev.2012.11.028

Conflict of Interest Statement: The authors declare that the research was conducted in the absence of any commercial or financial relationships that could be construed as a potential conflict of interest.

Copyright © 2018 Limoges, Massé, Weckström, Poulin, Ellegaard, Heikkilä, Geilfus, Sejr, Rysgaard and Ribeiro. This is an open-access article distributed under the terms of the Creative Commons Attribution License (CC BY). The use, distribution or reproduction in other forums is permitted, provided the original author(s) and the copyright owner(s) are credited and that the original publication in this journal is cited, in accordance with accepted academic practice. No use, distribution or reproduction is permitted which does not comply with these terms.